Four atom efficient enzyme cascades for all 4-methoxyphenyl-1,2-propanediol isomers including product crystallization targeting high product concentrations and excellent E-factors

Reinhard Oeggl [†], Tim Maßmann [‡], Andreas Jupke [‡], Dörte Rother [†,≠,]*

† IBG-1: Biotechnology, Forschungszentrum Jülich GmbH, Wilhelm Johnen Straße, 52425 Jülich, Germany

‡ AVT.Fluidverfahrenstechnik, RWTH Aachen University, Forckenbeckstraße 51, 52074 Aachen, Germany

≠ RWTH Aachen University, ABBt – Aachen Biology and Biotechnology, Worringerweg 1, 52074 Aachen, Germany

* corresponding author: Dörte Rother, do.rother@fz-juelich.de; Tel.: +49 2461 61-6772

Fax: +49 2461 61-

Index

S1. Initial activity measurements

Initial activities measurements were performed for solvent selection, substrate pulsing for carboligation optimization and co substrate selection for NADPH regeneration in the reduction. To ensure a linear measurement, it was assumed that within the first 10 % of converted substrate no limitation occurs. Measurements were conducted in the respective range. Initial activities were measured with substrate concentrations equal or similar to reaction conditions of the final optimized process. The reaction setup was carried out as follows: First the substrates were diluted in the respective organic solvent. The solution was added to the lyophilized whole cells (LWC). Then, the reaction was started by buffer addition.

S2. Green solvent implementation in a micro-aqueous reaction system

In MARS, a lyophilized whole cell catalyst is submerged in substrates dissolved in organic solvent with buffer to ensure catalytic activity. Sensible solvent selection is essential to ensure best catalytic activity of hydrophilic enzymes in this hydrophobic system. The selection also impacts appropriate buffer amounts, because solvents take up different buffer amounts upon saturation.[1–3] Accordingly, four green solvents were selected to ensure a realistic time frame for the experimental procedure: MTBE[1,4], CPME[2,5,6], MTHF[6,7] and MIBK[8]. The choice was based on solvents, which are known to promote biocatalysis in combination with the selected biocatalysts.[1,4,5] Every solvent was screened empirically for optimal buffer contents to ensure best catalytic activities in a tedious process (data not provided).

In the experimental data the solvent CPME displayed the best initial activities with the catalysts *Pf*BAL and RADH. (Figure S1) For both catalysts, MTBE performed second-best. The other two catalysts, *Pp*BFD varL461A and *Lb*ADH, displayed the highest catalytic activity in MTBE and the second-best activity in CPME. Interestingly, all catalysts were unable to achieve even a third of the specific initial activity in MTHF and MIBK than in the best-performing ether. These findings suggest combined with observation by others that ethers are in general biocatalysis promoting.[9] In consideration of the CHEM21 guidelines CPME was selected over MTBE. MTBE was recently identified as having potential safety and environmental risks.[8,10,11] In contrast, CPME is considered safe by the same guidelines. Moreover, its synthesis from renewable feedstock accounts for ecological implications.[2,8] In conclusion, CPME is the favored solvent for this cascade, due to biocatalysis promoting characteristics and ecological friendliness.

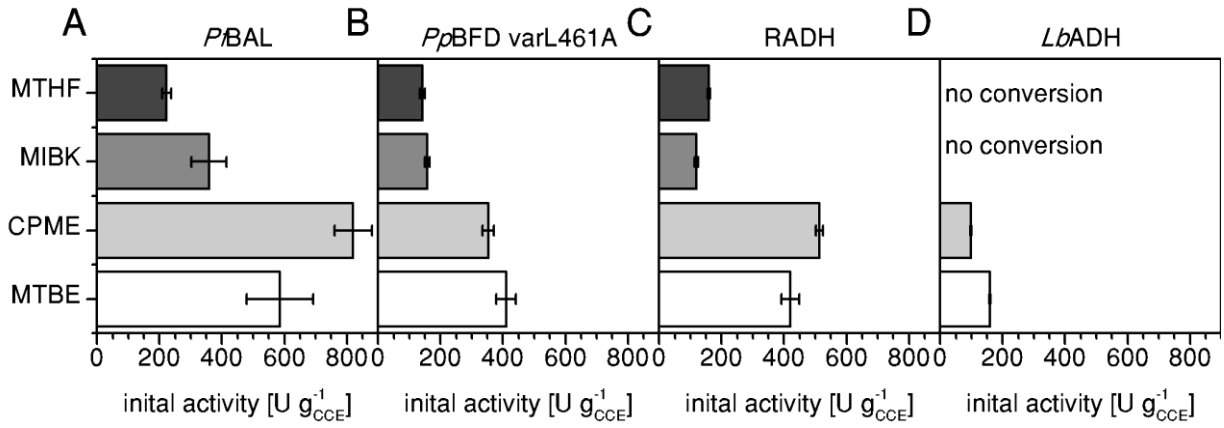

Figure S1. Specific initial enzyme activity in different green solvents. Initial activities of *Pseudomonas fluorescence* benzaldehyde lyase (*Pf*BAL) (A), *Pseudomonas putida* benzoylformate decarboxylase variant L461A (*Pp*BFD var461A) (B), *Ralstonia sp.* alcohol dehydrogenase (RADH) (C) and *Lactobacillus brevis* alcohol dehydrogenase (*Lb*ADH) (D) in four different organic solvents at 30 °C and 1000 rpm. Initial activities for BAL and BFD were measured using 500 mM 4-methoxy benzaldehyde and 180 mM acetaldehyde (BAL) or 120 mM acetaldehyde (BFD). RADH and *Lb*ADH activity was measured with 400 mM (*R*)-4-methoxyphenyl-1-propanone and 1 M cyclohexanol; MTHF (2-methyltetrahydrofuran), MIBK (methyl isobutyl ketone), CPME (cyclopentyl methyl ether), MTBE (methyl tert-butyl ether); n.c. … no conversion; n=3;

S3. Optimal aldehyde starting concentration for carboligation step

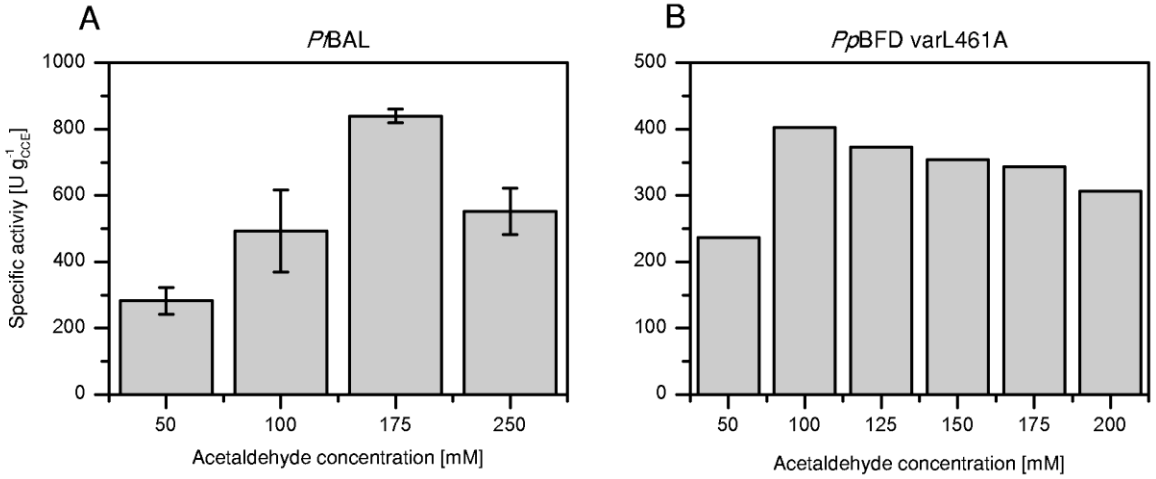

Figure S2. Optimal acetaldehyde starting conditions screened for *Pseudomonas fluorescences* benzaldehyde lyase (*Pf*BAL) and *Pseudomonas* putida benzoylformiat decarboxylase variant L461A (*Pp*BFD varL461A) reaction targeting (*R*)-4-methoxyphenyl-2-hydroxy-propanone formation in a micro aqueous reaction system. (A): The optimal starting concentration of acetaldehyde when paired with 500 mM 4-methoxy-benzaldehyde was screened in cyclopentyl methyl ether with 25 µg mL^{-1} *Pf*BAL lyophilized whole cells. 25 µL mL^{-1} 1 M TEA buffer pH 10 were added to start the reaction; 30 °C and 1000 rpm; analyzed with HPLC; n = 3; (B): The optimal starting concentration of acetaldehyde when paired with 500 mM 4-methoxy-benzaldehyde was screened in cyclopentyl methyl ether with 100 µg mL^{-1} *Pp*BFD varL461A lyophilized whole cells. 100 µL mL^{-1} 1 M TEA buffer pH 10 were added to start the reaction; 30 °C and 1000 rpm; analyzed with HPLC; n = 1

S4. Acetaldehyde pulsing in the first cascade step

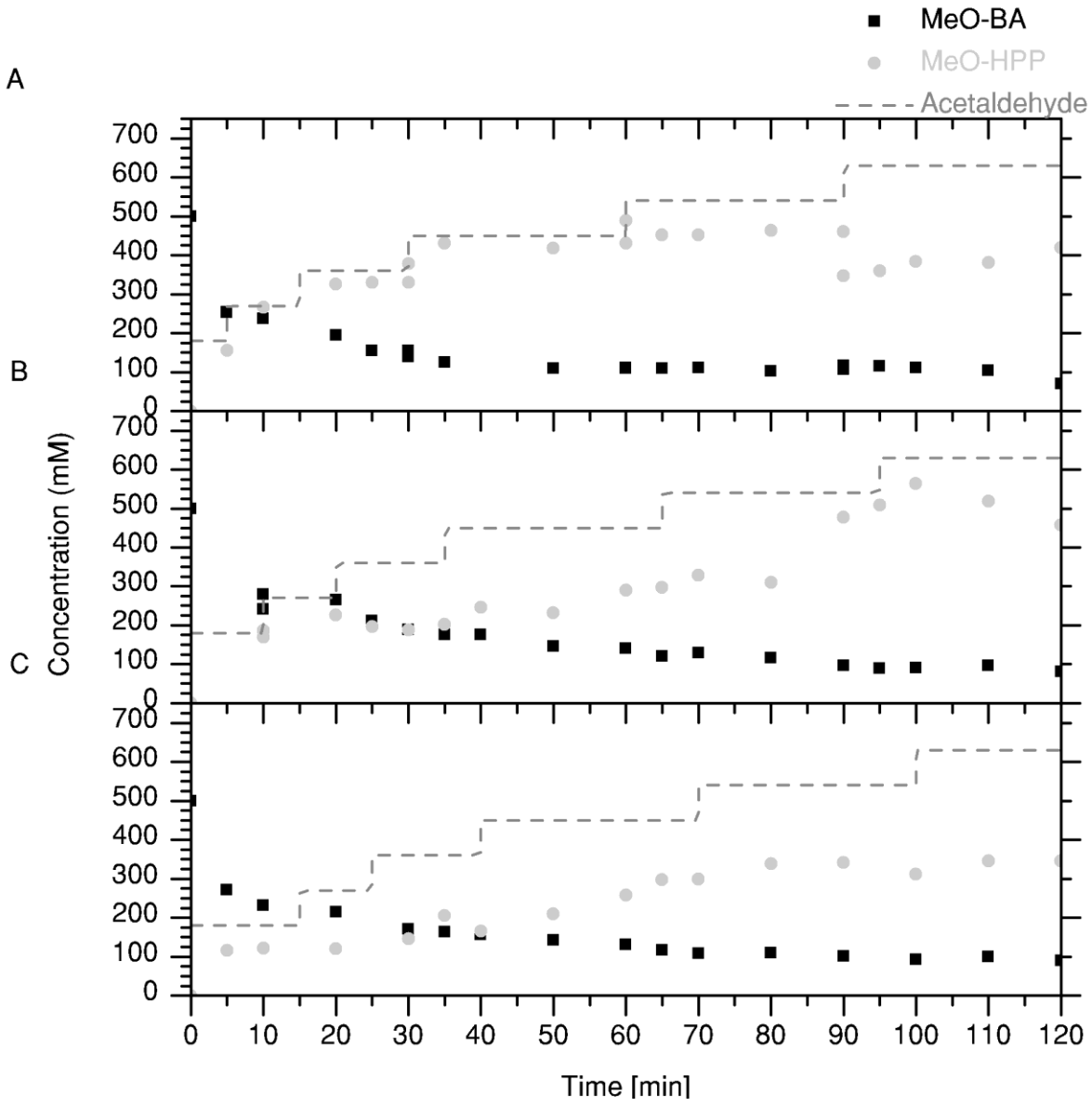

Figure S3. Stepwise feeding of acetaldehyde in a micro aqueous reaction system with *Pseudomonas fluorescence* benzaldehyde lyase (*Pf*BAL). Acetaldehyde was pulsed to the starting conditions to achieve an optimal space-time-yield. Starting concentrations: 500 mM 4-methoxy-benzaldehyde and 180 mM acetaldehyde and 25 mg mL^{-1} *Pf*BAL lyophilized whole cells with 25 µL mL^{-1} 1 M TEA buffer pH 10 in cyclopentyl methyl ether. 90 mM acetaldehyde were pulsed at the indicated points in time; 30 °C, 1000 rpm; A: 180 mM Acetaldehyde added within 15 min, B: 180 mM acetaldehyde added within 20 min , C, 180 mM acetaldehyde added within 25 min; analyzed with HPLC, n = 1

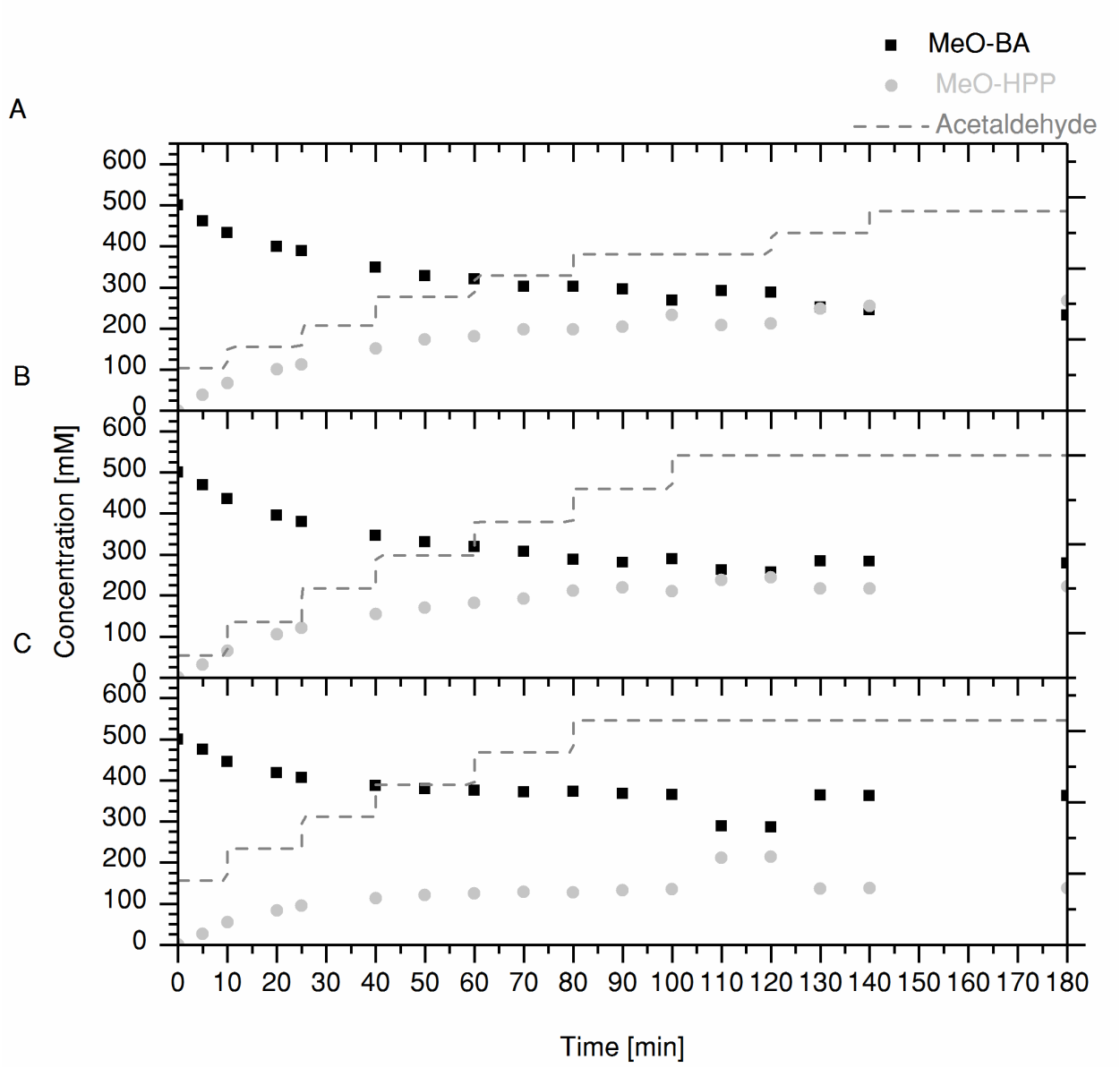

Figure S4. Stepwise feeding of different acetaldehyde concentrations in the same interval in a micro aqueous reaction system with *Pseudomonas putida* benzoylformiat decarboxylase variant L461A (*Pp*BFD L461A). Acetaldehyde was pulsed to the starting conditions to achieve an optimal space-time-yield. Starting concentrations: 500 mM 4-methoxy-benzaldehyde and varying concentrations of acetaldehyde and 100 mg mL^{-1} *Pp*BFD varL461A lyophilized whole cells with 100 µL mL^{-1} 1 M TEA buffer pH 10 in cyclopentyl methyl ether. Pulsed were 60 mM acetaldehyde at the indicated points in time. 30 °C A: 120 mM acetaldehyde and 60 mM pulses, B: 150 mM acetaldehyde and 75 mM pulses, C, 180 mM acetaldehyde and 80 mM pulses; reaction was incubated at 30 °C and 1000 rpm; analyzed with HPLC; n = 1

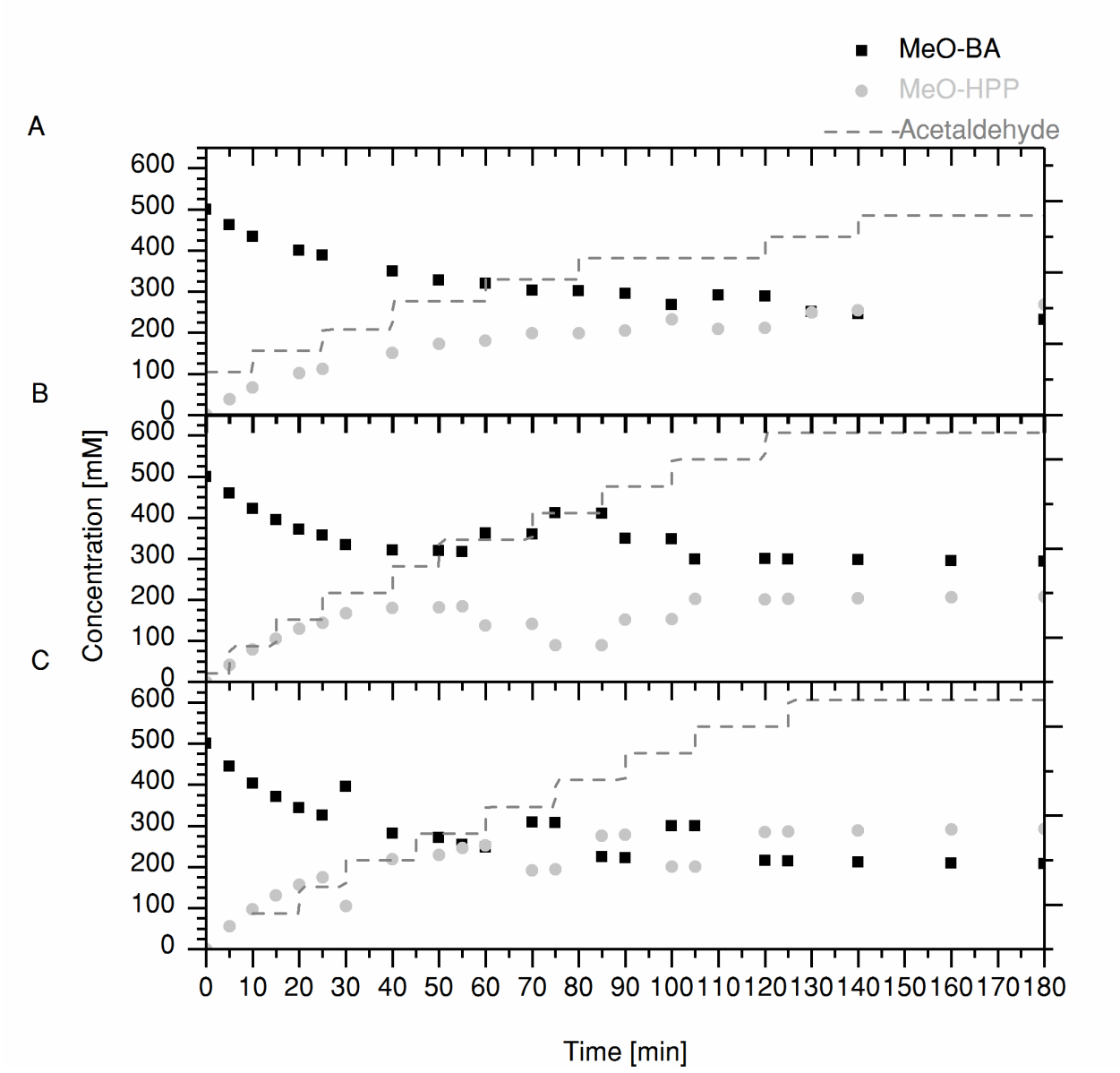

Figure S5. Stepwise feeding of acetaldehyde in alternating intervals to a micro aqueous reaction system with *Pseudomonas putida* benzoylformiat decarboxylase variant L461A (*Pp*BFD varL461A). Acetaldehyde was pulsed to the starting conditions to achieve an optimal space-time-yield. 500 mM 4-methoxy-benzaldehyde and 180 mM acetaldehyde and 100 mg mL^{-1} *Pp*BFD L461A lyophilized whole cells with 100 µL mL^{-1} 1 M TEA buffer pH 10 in cyclopentyl methyl ether. pulsed were 60 mM acetaldehyde at the indicated points in time. 30 °C, 1000 rpm; A: 180 mM acetaldehyde pulsed in 25 min, B: 180 mM acetaldehyde pulsed in 15 min, C, equal interval as A, but break after 1 h analyzed with HPLC; n = 1

S5. Evaluation of optimal co-substrate concentrations for the reductive step

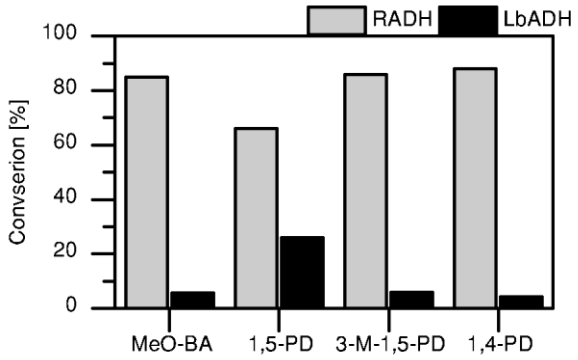

Figure S6. 1 N auxiliary substrate comparison for both alcohol dehydrogenase steps. Smart co-substrates were compared against a substrate for a self-sufficient cascade in regards of conversion after 24 h. Reaction conditions: 30 mg mL^{-1} LWC (either RADH or *Lb*ADH) with 45 µL mL^{-1} 1 M TEA buffer pH 10 for RADH or 15 µL mL^{-1} of the same buffer for *Lb*ADH; 400 mM (*R*)-hydroxy-phenyl-propanone; 1 M 1,5-pentanediol (1,5-PD), 1 M 3-methyl-1,5-pentanediol (3-M-1,5-PD), 1 M 1,4-pentanediol (1,4-PD) or 1 N 4-methoxy-benzylalcohol (MeO-BA); 30 °C; 1000 rpm; 24 h

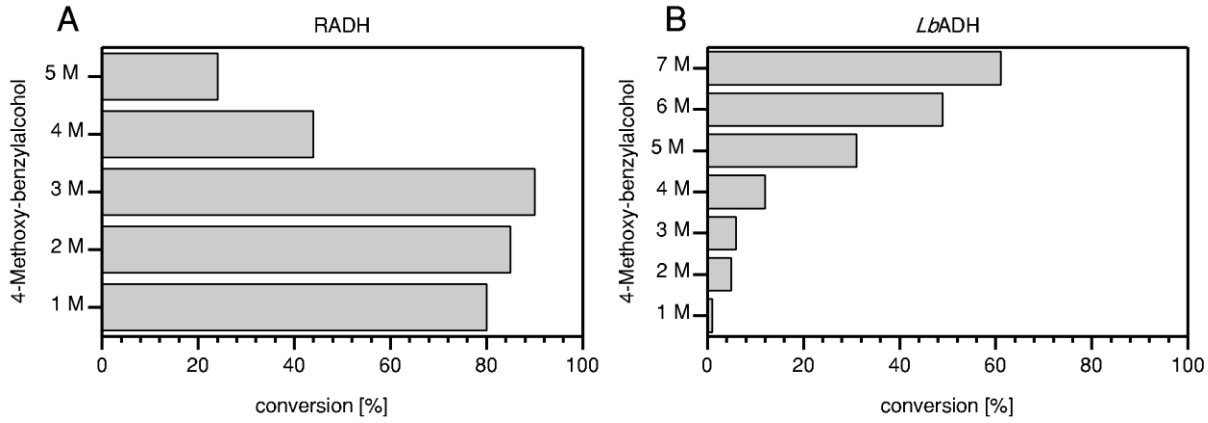

Figure S7. Conversion of 4-methoxyphenyl-2-hydroxy-propanone (MeO-HPP) to anethole-diol by applying different co-substrate concentrations. Two alcohol dehydrogenases (ADH) were investigated towards the formed amount of anethole-diol with different concentrations of 4-methoxy-benzylalcohol. The alcohol is applied to regenerate NADPH, which is required to reduce MeO-HPP. A: 30 mg mL^{-1} *Ralstonia sp.* ADH with 45 µL mL^{-1} 1 M TEA buffer pH 10 in cyclopentyl methyl ether with 400 mM MeO-HPP and the indicated amount of 4-methoxy-benzalcohol, reaction incubated at 30 °C and 1000 rpm for 6 h; B: 30 mg mL^{-1} *Lactobacillus brevis* ADH with 20 µL mL^{-1} 1 M TEA buffer pH 10 in cyclopentyl methyl ether with 400 mM MeO-HPP and the indicated amount of 4-methoxy-benzalcohol; 30 °C and 1000 rpm for 24 h; analyzed with GC; n = 1

S6. Cascade operation

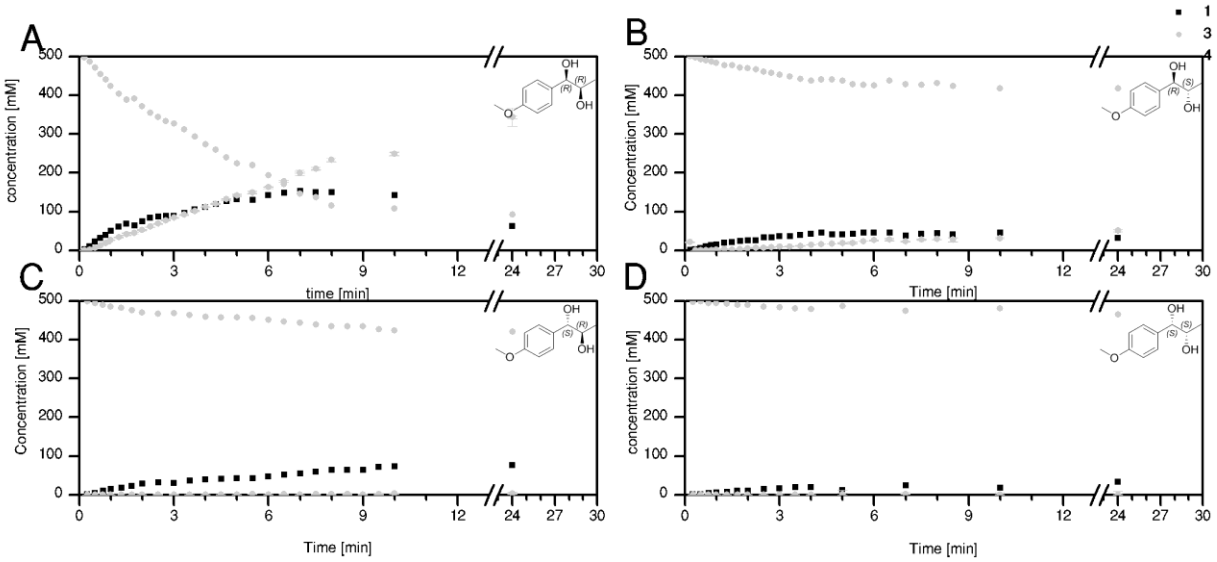

Figure S8. Anethole-diol production in a simultaneous enzyme cascade mode. carboligation and reduction take place at the same time in one pot. Hence both biocatalysts and all needed substrates are added from the beginning. Reaction conditions are listed according to the reaction type, First step: 25 mg mL^{-1} *Pseudomonas fluorescence* benzaldehyde lyase (PfBAL) lyophilized whole cells (LWC) were incubated with 500 mM 4-methoxy-benzaldehyde and 180 mM acetaldehyde in cyclopentyl methyl ether with 25 µL mL^{-1} 1 M TEA buffer pH 10. 90 mM acetaldehyde was dosed after 45 min, 100 min, 180 min, 240 min and 300 min; 100 mg mL^{-1} *Pseudomonas putida* benzoylformiat decarboxylase variant L461A (*Pp*BFD varL461A) were incubated with 500 mM 4-methoxy-benzaldehyde and 120 mM acetaldehyde in cyclopentyl methyl ether with 100 µL mL^{-1} 1 M TEA buffer pH 10. 90 mM Acetaldehyde was dosed after 50 min, 120 min, 180 min, 240 min, 300 min; 360 min, 420 min and 480 min; also from the beginning added was the corresponding alcohol dehydrogenase. Hence the following components were also added from the start: : 30 mg mL^{-1} *Ralstonia sp.* LWC were added to the reaction solution with 45 µL mL^{-1} 1 M TEA buffer Ph 10 and 3 M 4-methoxy-benzylalcohol; 90 mg mL^{-1} *Lactobacillus brevis* ADH (*Lb*ADH) were added with 60 µL mL^{-1} 1 M TEA buffer pH 10 and 5 M 4-methoxy-benzylalcohol to the reaction solution; reactions were incubated at 30 °C and 1000 rpm; n=3; analyzed with HPLC and GC;

Table S1. Conversions in each biocatalytic step in a sequential mode

	Conversion [%]		
	1st step	2nd step	overall
*Pf*BAL-RADH	79.1	90.0	71.2
*Pf*BAL-*Lb*ADH	79.1	47.0	37.2
*Pp*BFD varL461A-RADH	46,3	90.0	41.7
*Pp*BFD varL461A-*Lb*ADH	46,3	41.7	19.2

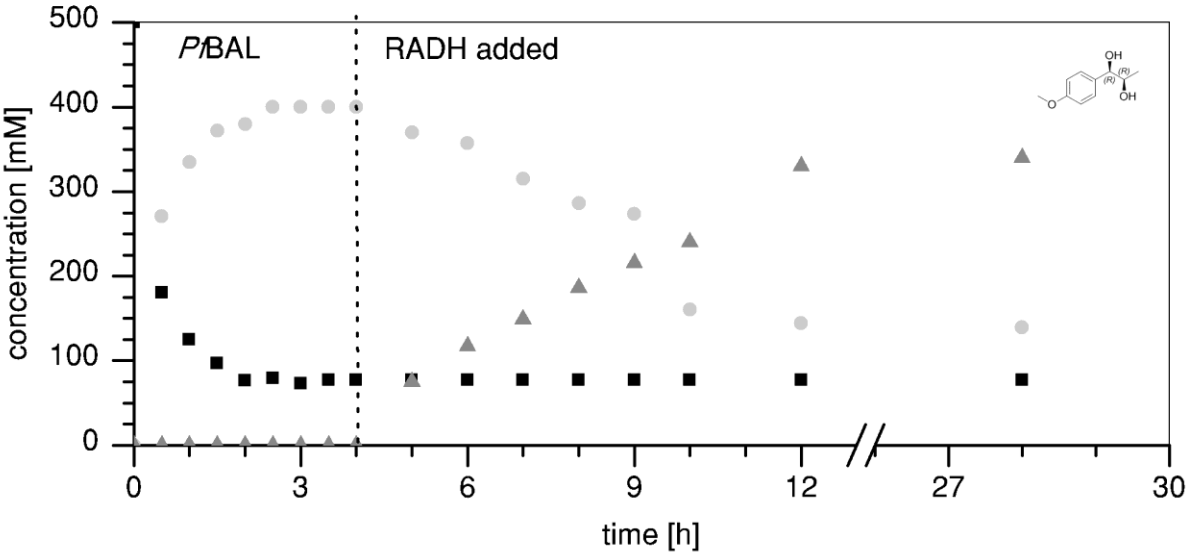

Figure S9. Preparative scale of (1*R*,2*R*)-anethole-diol. (1*R*,2*R*)-Anethole-diol was prepared in sequential mode. First, 25 mg mL^{-1} *Pseudomonas fluorescence* benzaldehyde lyase (*Pf*BAL) were incubated in a 500 mL pot with 500 mM 4-methoxy-benzaldehyde and 180 mM acetaldehyde in cyclopentyl methyl ether with 30 µL mL^{-1} 1 M TEA buffer pH 10. 90 mM Acetaldehyde was dosed after 10 min, 30 min, 45 min, 60 min and 90 min. After 4 h, 45 mg mL^{-1} *Ralstonia sp.* alcohol dehydrogenase (RADH) was added with 45 µL mL^{1} 1 M TEA buffer pH 10 and 3 M 4-methoxy-benzylalcohol. The reaction was incubated at 30 °C and 200 rpm. 4-methoxy-benzaldehyde (■), 4-methoxyphenyl-2-hydroxy-propanone (●), 4-methoxyphenyl-propanedioll (▲)

S7. Equations to calculate atom efficiency and environmental impact

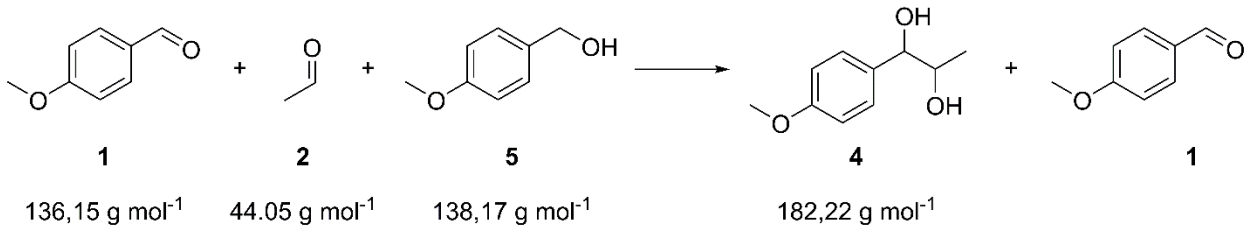

Figure S10. Reaction scheme of all educts and products to form 4-methoxyphenyl-propanedioll. displayed are all educts starting from 4-methoxy-benzaldehyde (**1**), acetaldehyde (**2**), 4-methoxy-benzylalcohol (**5**), and products 4-methoxyphenyl-propanedioll (**4**), and **1;**

Equation S1. Atom economy

$$AE = \frac{\sum MW(desired\ product)}{\sum MW(educts)} * 100$$

AE	atom economy [%]
MW	molecular weight [g mol^{-1}]

Equation S2. E-factor calculation:

$$E - factor = \frac{\sum m(waste)}{\sum m(product)}$$

E-factor	environmental factor [-]
m	mass [g]

Table S2. Raw data for the calculation of the E-factor. All numbers are normalized to a volume of 1 L

	Solvent [kg]	Substrate [kg]	Product [kg]
(1*R*,2*R*)-4	0.3203	0.5104	0.0600
(1*R*,2S)-4	0.3160	0.5090	0.0339
(1*S*,2*R*)-4	0.0429	0.7590	0.00374
(1*S*,2*S*)-4	0.0386	0.7590	0.01747

Table S3. Collected ecologic values

	Isomer	(1*R*,2*R*)	(1*S*,2*R*)	(1*R*,2*S*)	(1*S*,2*S*)
Sequential cascade	*atom economy [a] [%]*			57.2	
	E-factor [c] [-]	13.8	21.4	24.3	45.6
	E-factor with reaction solution recycling [d] [-]	< 1	n.a.	n.a.	< 1
Simultaneous cascade	*atom economy [b] [%]*			99.9	
	E-factor [c] [-]	12.3	n.a.	n.a.	n.a.
	E-factor with reaction solution recycling [d] [-]	< 1	n.a.	n.a.	n.a.

[a] The atom efficiency in sequential mode is calculated taking all substrates into account (acetaldehyde, 4-methoxy-benzaldehyde and 4-methoxy-benzylalcohol), whereas [b] the simultaneous cascade just relies on acetaldehyde and 4-methoxy-benzylalcohol. [c] The E-factor accounts for all required substrates, catalysts and solvents in the reaction and downstream processing in relation to the synthesized product diol. [d] An estimation that takes a possible direct recycling of the reaction solution after product crystal removement into account for the generated amount of waste. Notably, the crystallization was demonstrated for the enantiomer **(1*R*,2*R*)-4**. Thus it is assumed that the isomer **(1*S*,2*S*)-4** behaves in the same manner. For the two other isomers no predictions are made based on existing data; n.a. (not applicable)

S8. Product crystallization modelling for efficient downstream processing

Notably, all four isomers were successfully synthesized in the upstream process with conversions of up to 71 % (for conversions of each step see Figure S12). Now a selective product isolation of the product diol **4** from the remaining substrate **1** and **2**, co-substrate **5**, intermediate **3**, and solvent CPME by crystallization was envisaged. It was assumed that **1** and **2** can easily be removed by evaporation. The remaining co-substrate **5** acts as solvent and forms a solvent mixture with CPME. In this solvent mixture the similar physico-chemical behavior of the product **4** and the remaining intermediate **3** challenge a selective product isolation. This challenging is targeted by predicting the thermodynamics of 3&4 in the multi-component liquid phase. Thereby, identifying an optimal operational zone for product crystallization.

First, experimental data of both compound **3** and **4** in the two pure solvents, CPME and **5**, were used to determine their solubility with a simplified Schröder-van-Laar plot (Figure 5). Accordingly, both intermediate **3** and product **4** exhibit a solubility of > 250 g $L_{solvent}^{-1}$ at 35 °C in both CPME and **5**. Advantageously, the product **4** was determined to have half the solubility of **3** in CPME. This favors a selective crystallization of **4** and increases the potential yield of the downstream process.

In the next step, product crystallization under real reaction conditions was investigated. A supersaturation of the product in the mother liquor is targeted. In a first evaporation step at 50° C most of the CPME, remaining levels of substrates **1** and **2** were successfully removed. Only neglectable amounts of other compounds (**3**, **4**, and **5**) evaporated in this step. This implies an accumulation of the intermediate **3** and product **4** in a solvent mixture of CPME and predominantly the co-substrate **5**. In pure co-substrate **5**, the solubility gap between **3** and **4** declines especially at lower temperatures (grey lines vs black lines between plots A and B Figure 5 and Figure S13). Fortunately, **4** remains less soluble than **3**, enabling a selective product crystallization.

To predict the crystallization behavior the product **4** in a solvent mixture of CPME and **5**, its solid-liquid equilibrium from the Schröder-van-Laar plot was calculated in different solvent mixture ratios with the aid of COSMOthermX17 (Figure 5). Calculations were performed at 25 °C, because the solubility gap between **3** and **4** increases at lower temperatures. Lower temperatures were not applicable due to the relatively high melting point of **5** (T_m = 23 °C).

Due to the large difference in the obtained substance properties of the product diol **4** in CPME and **5** (Figure S12-A), the calculated solubilities by COSMOthermX17 differed drastically in pure CPME or pure **5** (Figure 5). The resulting solubility was approximated by multiplication of the solubility for each parameter set with the respective loading of CPME (I) and **5** (II) in the solvent (Figure 5 grey curves).

In the following the simulation predicted that a supersaturation for both individual compounds, the intermediate **3** and the product **4**, is achieved at the same concentration level. Advantageously, the model also studied interactions of both compounds **3** and **4** in the solvent mixture. Thus, an

accumulation of intermediate **3** decreases the solubility of the product diol **4** (Figure 5), which facilitates a selective product crystallization of the diol **4** in the model. Thus, the model was able to identify suitable conditions for a selective product crystallization.

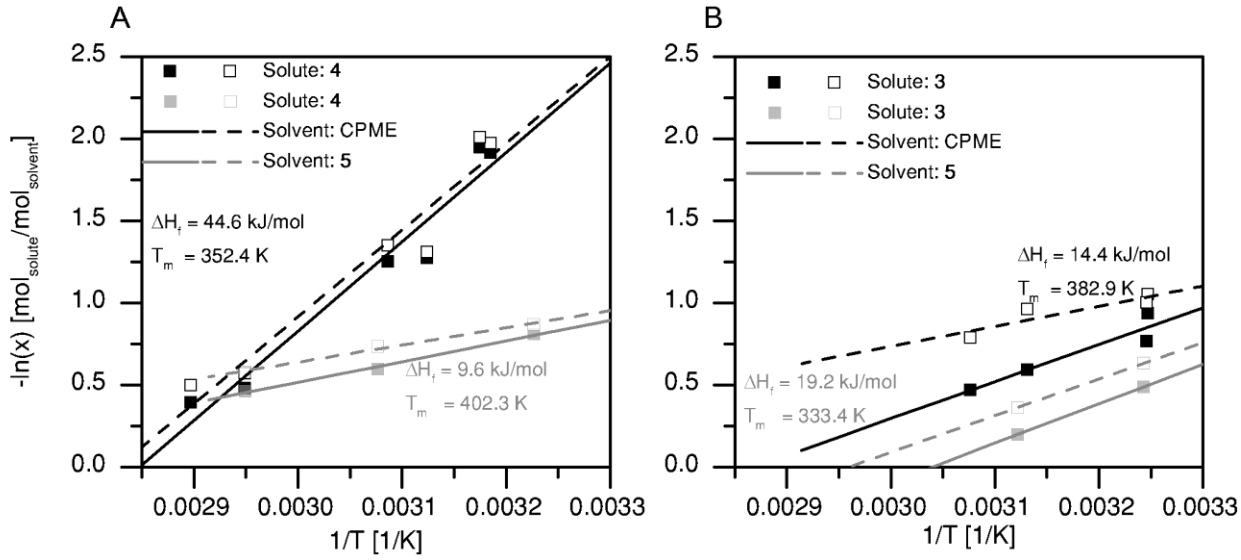

Figure S11. Experimental solubility data for the product diol 4 (A), and the intermediate 3 (B), in CPME (black) and 5 (grey) individually shown in a simplified Schröder-van-Laar plot. Full symbols show the upper boundary of the solubility area, open symbols show the lower boundary. Property data is averaged between the linearization for the upper and lower boundary.

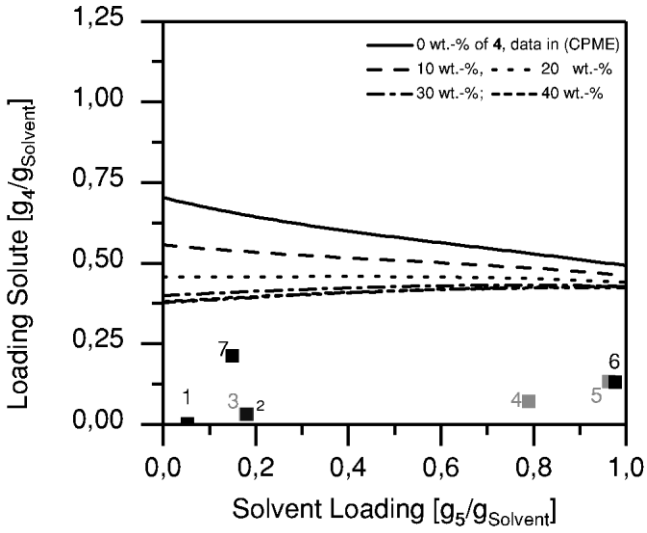

Figure S12. Solubility calculated by COSMOthermX17 for the intermediate 3 in the quaternary system with CPME and 5 for different % (w w^{-1}) of the other substance 3 or 4 in solution at 25 °C. The symbols show solvent composition after different process steps. 1. Feed to enzyme cascade, 2. Product of enzyme cascade, 3. First crystallization of 5, 4. After evaporation at 50° C and attempted crystallization of 5, 5. After evaporation at 100° C, 6. Mother solution after cooling crystallization of 4 to 25° C, 7. Crystal-enriched phase after centrifugation.

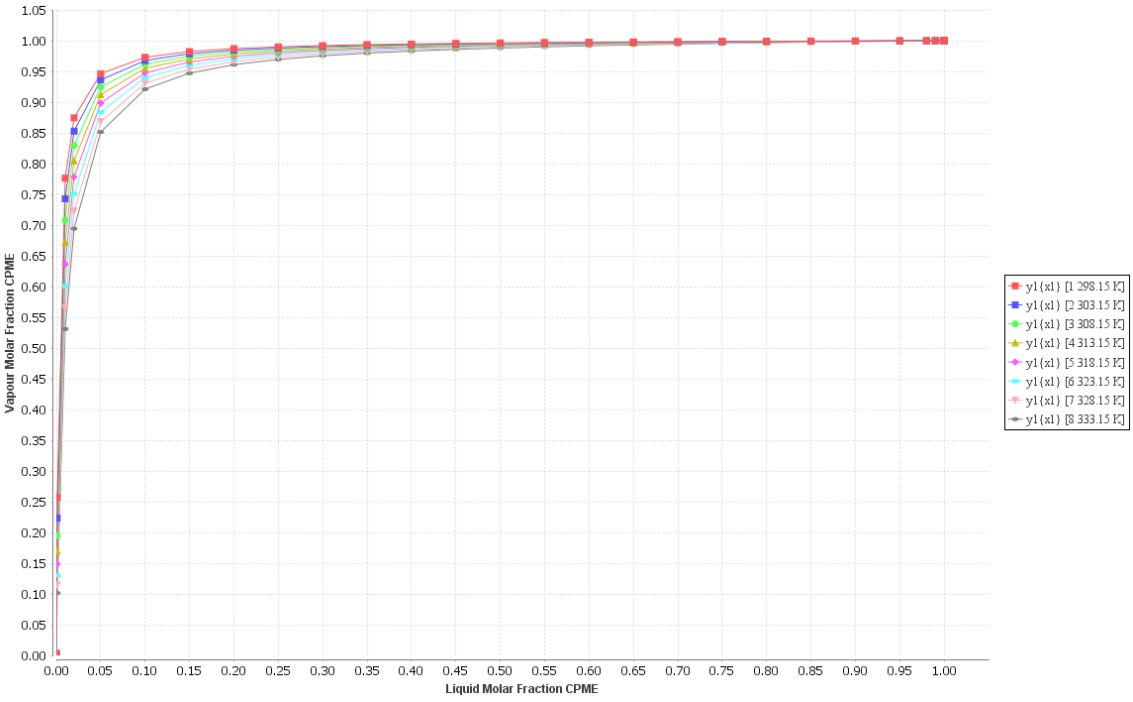

Figure S13. Vapour-liquid-equilibria data of (1*R*,2*R*)-4 in CPME and 5 approximated by cosmothermX17

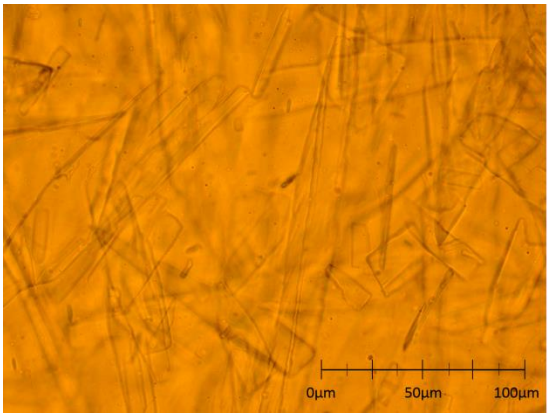

FigureS14. Picture from microscope of crystal phase after cooling crystallization and solid separation by centrifugation.

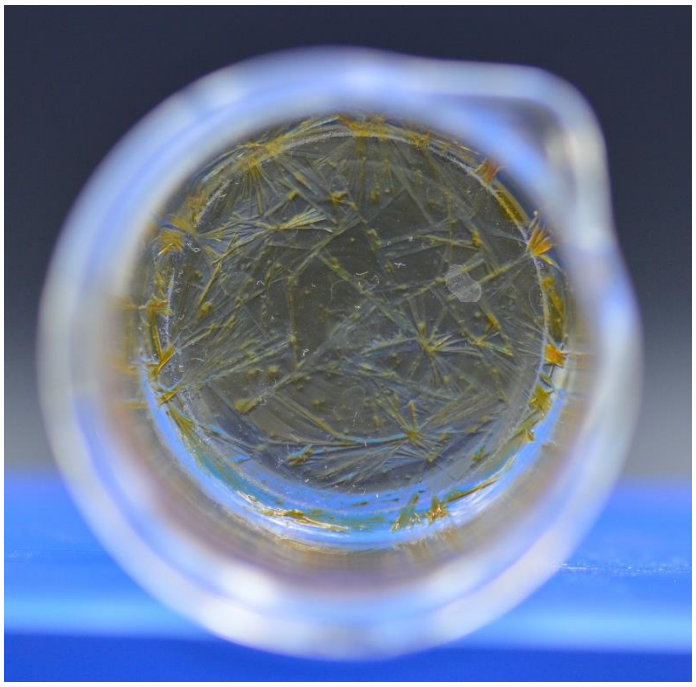

Figure S15. Picture of crystals obtained after recrystallization from acetone and vacuum drying showing needle form of crystals as seen in figure 15 under the microscope.

S9. 1H NMR spectra from all four product isomers

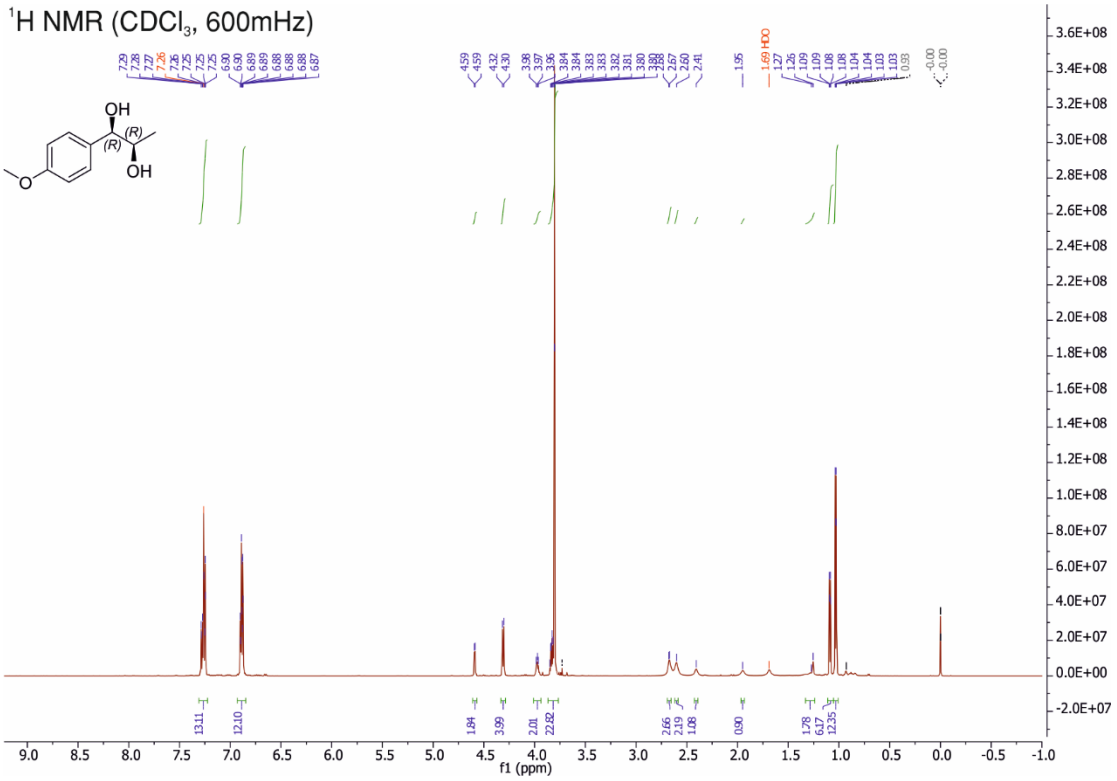

Figure S16. ^{1}H NMR of (1*R*,2*R*)-4-methoxyphenyl-propanediol:

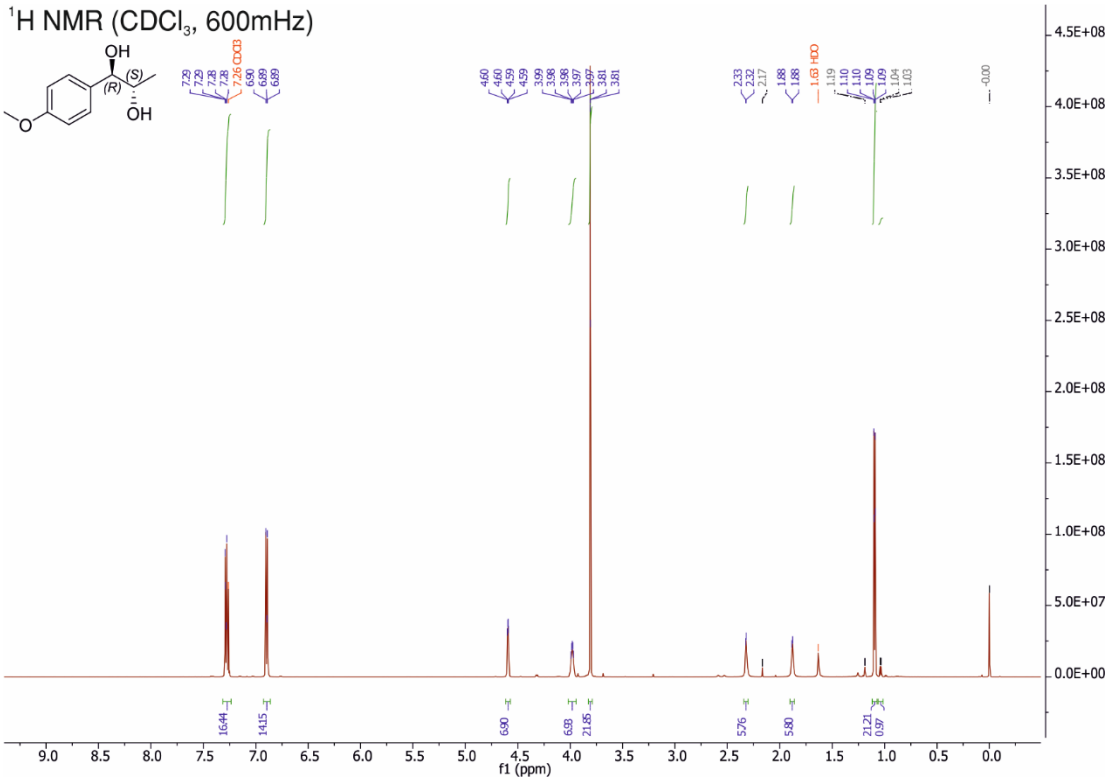

Figure S17. ^{1}H NMR of (1*R*,2*S*)-4-methoxyphenyl-propanediol:

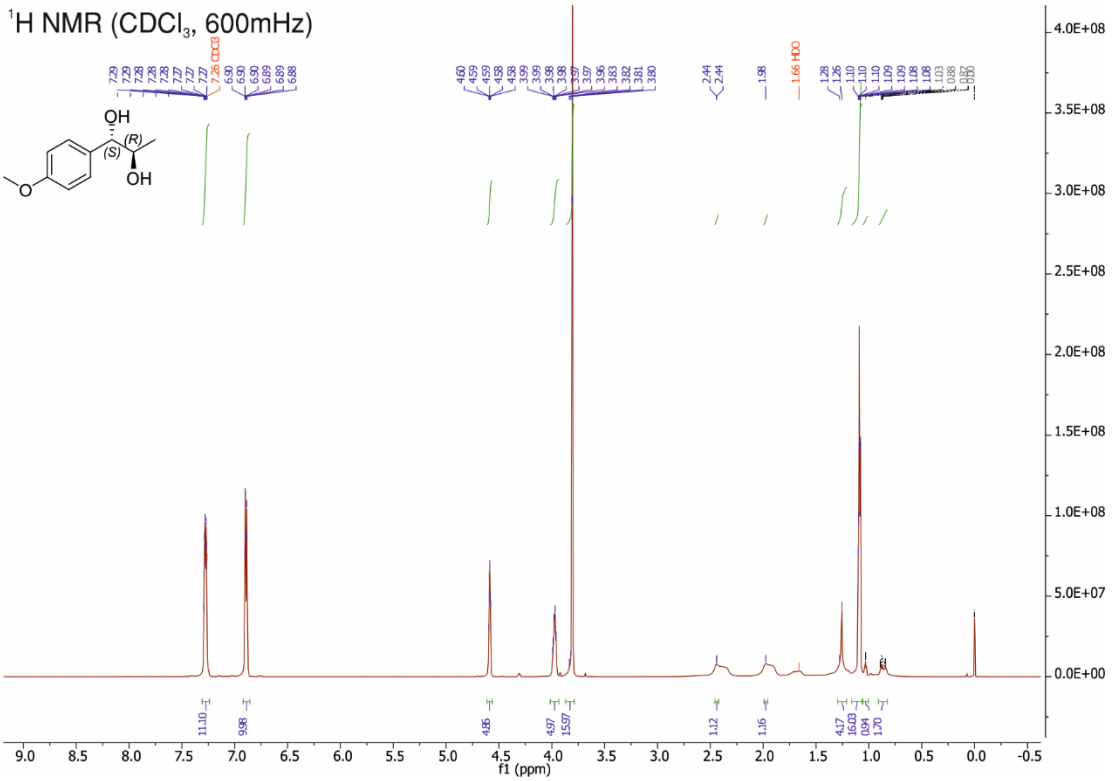

Figure S18. ^{1}H NMR of (1*S*,2*R*)-4-methoxyphenyl-propanediol:

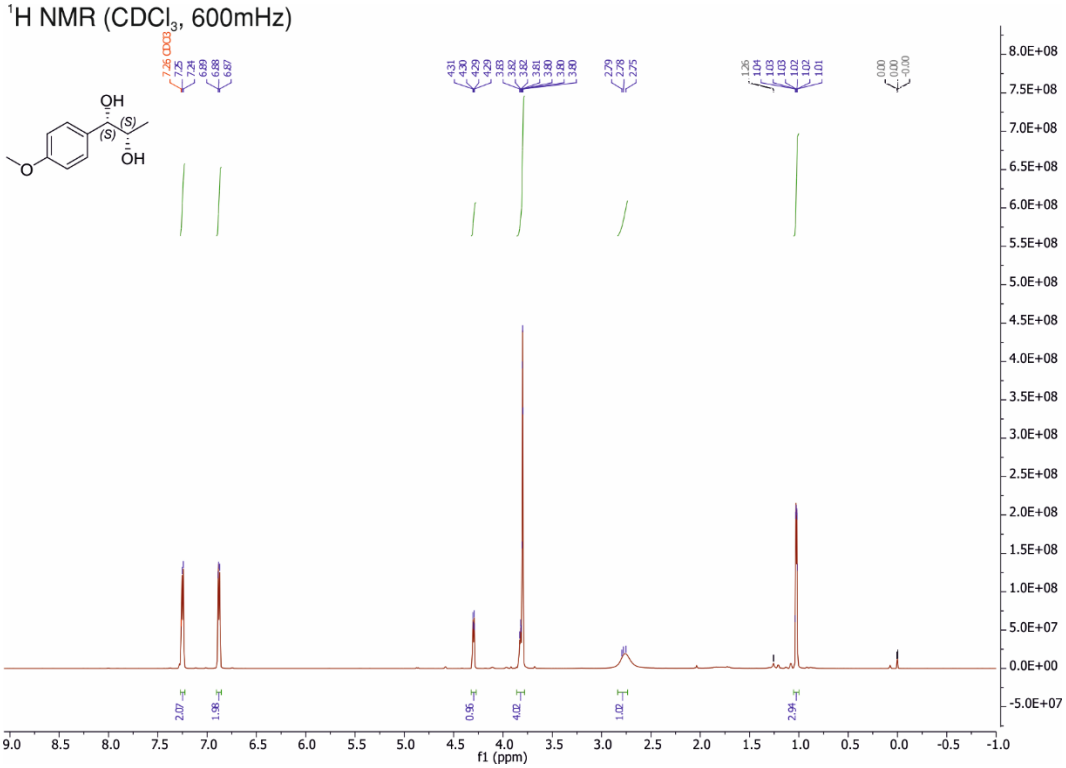

Figure S19. ^{1}H NMR of (1*S*,2*S*)-4-methoxyphenyl-propanediol.

References

(1) Jakoblinnert, A.; Rother, D. A Two-Step Biocatalytic Cascade in Micro-Aqueous Medium: Using Whole Cells to Obtain High Concentrations of a Vicinal Diol. *Green Chem.* **2014**, *16* (7), 3472–3482.

(2) Watanabe, K.; Yamagiwa, N.; Torisawa, Y. Cyclopentyl Methyl Ether as a New and Alternative Process Solvent. *Org. Process Res. Dev.* **2007**, *11* (2), 251–258.

(3) Wachtmeister, J.; Mennicken, P.; Hunold, A.; Rother, D. Modularized Biocatalysis: Immobilization of Whole Cells for Preparative Applications in Microaqueous Organic Solvents. *ChemCatChem* **2016**, *8* (3), 607–614.

(4) Wachtmeister, J.; Jakoblinnert, A.; Rother, D. Stereoselective Two-Step Biocatalysis in Organic Solvent: Toward All Stereoisomers of a 1,2-Diol at High Product Concentrations. *Org. Process Res. Dev.* **2016**, *20* (10), 1744–1753.

(5) Maugeri, Z.; Rother, D. Application of Imine Reductases (IREDs) in Micro-Aqueous Reaction Systems. *Adv. Synth. Catal.* **2016**, *358* (17), 2745–2750.

(6) Sheldon, R. A. Fundamentals of Green Chemistry: Efficiency in Reaction Design. *Chem. Soc. Rev.* **2012**, *41* (4), 1437–1451.

(7) Chapter 5. Renewable Solvents. In *Alternative Solvents for Green Chemistry*; Royal Society of Chemistry: Cambridge, 2009; pp 97–117.

(8) Prat, D.; Wells, A.; Hayler, J.; Sneddon, H.; McElroy, C. R.; Abou-Shehada, S.; Dunn, P. J. CHEM21 Selection Guide of Classical- and Less Classical-Solvents. *Green Chem.* **2016**, *18* (1), 288–296.

(9) Filho, M. V.; Stillger, T.; Müller, M.; Liese, A.; Wandrey, C. Is LogP a Convenient Criterion to Guide the Choice of Solvents for Biphasic Enzymatic Reactions? *Angew. Chemie - Int. Ed.* **2003**, *42* (26), 2993–2996.

(10) Saeedi, A.; Omidi, M.; Khoshnoud, M. J.; Mohammadi-Bardbori, A. Exposure to Methyl Tert-Butyl Ether (MTBE) Is Associated with Mitochondrial Dysfunction in Rat. *Xenobiotica* **2017**, *47* (5), 423–430.

(11) Roslev, P.; Lentz, T.; Hesselsoe, M. Microbial Toxicity of Methyl Tert-Butyl Ether (MTBE) Determined with Fluorescent and Luminescent Bioassays. *Chemosphere* **2015**, *120*, 284–291.